

Corrosion behavior of hypereutectic Al-23%Si alloy (AC9A) processed by severe plastic deformation

JIANG Jing-hua(江静华)¹, MA Ai-bin(马爱斌)¹, SONG Dan(宋丹)¹,
N. SAITO², YUAN Yu-chun(袁玉春)¹, Y. NISHIDA²

1. College of Materials Science and Engineering, Hohai University, Nanjing 210098, China;

2. National Institute of Advanced Industrial Science and Technology, 2266-98, Anagahora, Shimoshidami,
Moriyama-ku, Nagoya 463-8560, Japan

Received 21 November 2008; accepted 19 May 2009

Abstract: Ultrafine-grained(UFG) hypereutectic Al-23%Si (mass fraction) alloy was achieved through equal-channel angular pressing(ECAP) procedure. And the electrochemical properties after various ECAP passes were investigated in neutral NaCl solution. Potentiostatic polarization curves show that the corrosion potential of the ECAPed sample after 4 passes decreases markedly, while the corrosion current density reaches 1.37 times that of the as-cast alloy. However, the ϕ_{corr} and J_{corr} values after 16 passes are improved and approach those of the as-cast alloy. Immersion tests also show that the mass-loss ratio of ECAPed alloy decreases with increasing the pressing pass, which is lowered to 28.7% with the increase of pass number from 4 to 16. Pitting susceptibility of the ECAPed alloy after initial 4 passes is boosted, due to the presence of biggish voids resulted from the breakage of brittle large primary silicon crystals during ECAP. Increasing ECAP pass makes the voids evanesce and results in the homogeneous ultrafine-grained structure, contributing to a higher pitting resistance. These results indicate that enough ECAP passes are beneficial to increasing corrosion resistance of the hypereutectic Al-23%Si alloy.

Key words: aluminum casting alloys; ECAP; corrosion behavior; ultrafine grained microstructure

1 Introduction

Casting Al-Si alloys are found wide application for lightweight components in the automotive, aerospace and construction industries due to their good amenability to casting, high specific strength, superior corrosion resistance and low cost[1]. However, hypereutectic Al-Si alloy has a shortcoming, that is, its toughness remarkably decreases with increasing Si content. It is reasonable to anticipate that the toughness and wear resistance of hypereutectic Al-Si alloys with fine grains are improved[2–4]. So, one admitted approach is to fabricate ultrafine-grained(UFG) hypereutectic Al-Si alloy with fine primary silicon crystals and dispersed eutectic silicon particles.

ECAP is one of the most effective techniques for fabricating UFG metallic materials[5–8], which could endow exceptional mechanical or/and physical advantages without remarkably changing the geometry

of a bulk material[9–14]. Our previous study[15] indicated that the impact toughness of Al-23%Si (mass fraction) alloy after severe plastic deformation(SPD) by using an equal channel angular pressing with a rotary-die (RD-ECAP) was significantly increased, maximum 18 times higher than that of the as-cast alloy, due to the refinement of the grains (about 150 nm in diameter) and breakage of the primary and eutectic silicon crystals during ECAP. However, it was also noticed that some voids were presented after initial ECAP passes and evanesced with further more passes, which may affect the corrosion behavior and potential application of UFG Al-23%Si alloy.

It is noteworthy that recent investigations of ECAP processed(ECAPed) material mainly concerned structural characterization[5–8], mechanical properties [9–10], fatigue[11], creep[12], superplasticity[13], magnetic properties[14], etc. The corrosion behavior of the ECAPed materials has received only limited attention. Furthermore, these available results indicated that the

UFG effect on corrosion resistance varies in various alloy systems, such as UFG Cu[16], Ni[17], Ti[18] and Fe[19] alloys. Therefore, the systematic investigation and characterization of corrosion behavior for the ECAPed hypereutectic Al-Si alloy is important both for its possible engineering application and for the extension of current knowledge of the ECAP process. In the present work, an UFG Al-23%Si alloy processed by RD-ECAP was used for investigating the corrosion behaviors by electrochemical method, and the results were discussed and compared with the as-cast alloy.

2 Experimental

A hypereutectic Al-Si alloy (AC9A) was used with the composition of Al-23%Si-1%Cu-1%Mg-1%Ni (mass fraction). Except for the as-cast sample, three kinds of Al-23%Si samples with various ECAP pass number ($N=4, 8$ and 16 , respectively) were obtained to investigate the effect of changing microstructures on their corrosion behavior. Multi-pass ECAP was conducted using a rotary-die having a channel angle of 90° through Route A[20]. The RD-ECAP method is very easy to continuously process a bulk material sample[9] and one ECAP pass only needs 30 s. Considering the poor plasticity of Al-23%Si alloy even at elevated temperature, the samples for 4 and 8 passes were continuously pressed at a high temperature of (673 ± 6) K and another sample for 16 passes was processed at (623 ± 6) K, which are the same as those used in the previous work[15] for investigating its impact toughness. After multi-pass RD-ECAP, Al-23%Si alloy could obtain ultrafine grain or grain fragment (about 150 nm) [15]. Herein, microstructures of these samples were observed on a Nikon Eclipse ME600 optical microscope and the silicon particle size distribution was investigated by an image analysis system.

Corrosion samples were cut from the as-cast and as-ECAP billets (20 mm in diameter and 36 mm in length), and subsequently molded in epoxy resins of 20 mm in diameter and ground with 600-grit SiC paper. Referring to the various corrosion test standards[21], potentiostatic polarization tests were conducted at room temperature in 0.6 mol/L sodium chloride solution using an advanced electrochemical system of PARSTAT2273. This system was equipped with a reference electrode Hg-Hg₂Cl₂/saturated KCl (SCE), Pt counter electrode and Luggin capillary one. Prior to the potentiostatic polarization tests, each sample was immersed in the test solution to remove the natural oxide film for achieving a steady open circuit potential(OCP), which was measured as the corrosion potential(φ_{corr}). Polarization curve was obtained by potential sweeps of 1 mV/s, from which corrosion current was determined using the Tafel

extrapolation procedure. After polarization test, these corroded samples were observed by means of scanning electron microscopy(SEM) to analyze the corrosion mechanism of this alloy with and without ECAP processing. According to immersion method, the mass-loss ratio of ECAPed alloy was measured at room temperature in a 0.6 mol/L NaCl aqueous solution for 80 h.

3 Results and discussion

Fig.1 illustrates the optical micrographs of Al-23%Si alloy in various states, with (a), (b), (c) and (d) for the as-cast, 4-pass, 8-pass and 16-pass ECAPed sample, respectively. The size distribution of the silicon crystals in these samples is illustrated in Fig.2. It is obvious that many large polygonal primary silicon crystals with occasional voids (marked by arrows) are presented in the microstructures of the as-cast alloy (Fig.1(a)), except for many aluminum crystal dendrites and eutectic silicon dispersed in aluminum dendrite arms. After 4 passes, a large number of brittle primary silicon crystals are broken and many voids (with average size of about 50 μm) are formed around them (Fig.1(b)). After 8 passes of ECAP, the fragmentized primary silicon crystals and eutectic silicon included in the fine aluminum crystal are dispersed homogeneously; meanwhile, the average size of voids is noticeably decreased (Fig.1(d)). Evidently, most of the large primary silicon crystals are broken into relatively small particles after multi-pass ECAP (Fig.2). The refinement and homogenization of primary silicon particles lead to the gradual elimination of voids, since these voids are derived from the primary silicon particles (Fig.1(e)). Therefore, although some biggish silicon particles and small voids remain in the sample after 16 passes, their fraction is possible to be decreased through more passes of ECAP. Fig.1(f) presents that the number of voids and their average size are noticeably decreased after 32 passes, compared with the 4-pass sample (Fig.1(e)). The results indicate that a large pass RD-ECAP may weaken the pitting susceptibility of ECAPed Al-23%Si alloy, attributed to the gradual elimination of voids and the uniform distribution of fine secondary-phase particles on UFG Al matrix. CHUNG et al[22] found out that ECAPed AA1050 had smaller Si-containing impurities and reduced micro-galvanic currents due to its ultrafine-grained microstructure; and this alloy in ECAPed state had increased corrosion resistance with increasing ECAP pass number because of its small cathodic impurities. Likewise, for the ECAPed Al-23%Si alloy without voids, the uniform distribution of fine silicon particles in UFG Al matrix may reduce general micro-galvanic current and improve its corrosion resistance.

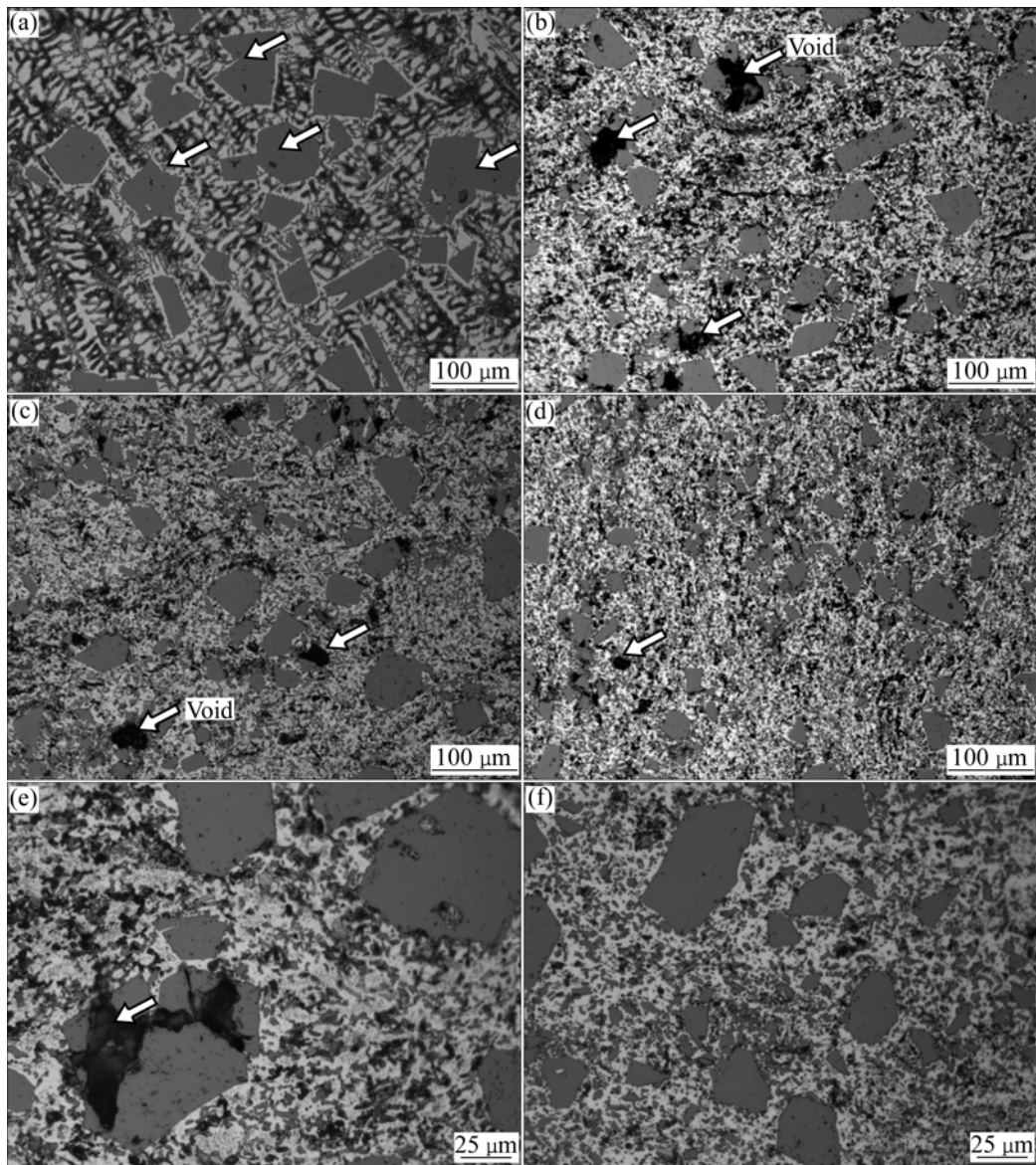


Fig.1 Optical micrographs of Al-23%Si alloy in various states: (a) as-cast; (b) ECAPed with 4 passes; (c) ECAPed with 8 passes; (d) ECAPed with 16 passes; (e) High magnification image of (b); (f) High magnification image of 32-pass ECAPed sample

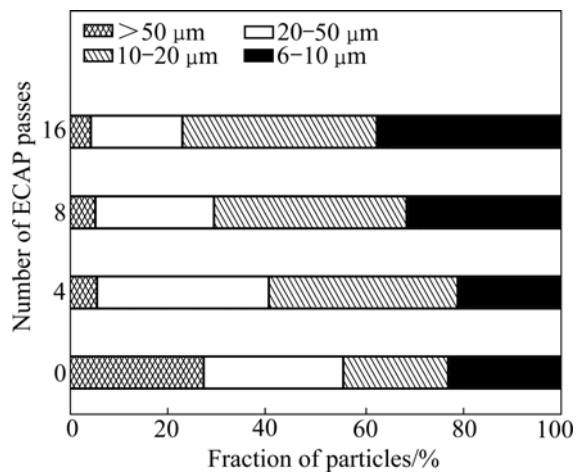


Fig.2 Distribution of silicon particles in Al-23%Si alloy in various states

The potentiostatic polarization curves of as-cast and ECAPed samples in 0.6 mol/L NaCl solution are shown in Fig.3, from which the corrosion potential(ϕ_{corr}) and corrosion current density(J_{corr}) are calculated and presented in Fig.4. Several interesting features can be deduced from these curves in Fig.3. 1) After 4 passes, corrosion potential of Al-23%Si alloy is lower than that of as-cast sample with coarse primary silicon crystals and its value of J_{corr} is 1.37 times higher than the latter, which is very different from the results obtained by BALYANOV et al[18], HADZIMA et al[19], and CHUNG et al[22]. 2) For the ECAPed Al-23%Si alloy with ultrafine-grained microstructure, ϕ_{corr} shifts toward the noble direction with increasing ECAP passes, while its corrosion current density declines accordingly. 3) After 16 passes, the values of ϕ_{corr} and J_{corr} for ECAPed

sample are close to those of as-cast alloy. These results clearly demonstrate that the corrosion resistance of ECAPed Al-23%Si alloy decreases in the initial pressing stage but is gradually improved after multi-pass ECAP. Corrosion resistance of ECAPed sample after 16 passes is close to that of the as-cast alloy. It can be deduced that corrosion resistance of the ECAPed Al-23%Si alloy would be further improved with increasing passes, due to homogeneous distribution of silicon particles in ultrafine-grained matrix and gradual elimination of voids around silicon particles.

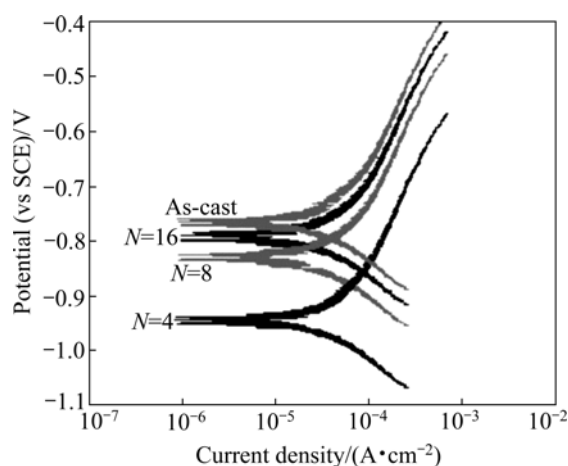


Fig.3 Potentiostatic polarization curves obtained from as-cast and ECAPed Al-23%Si alloy with various passes ($N=4, 8, 16$) in 0.6 mol/L NaCl solution

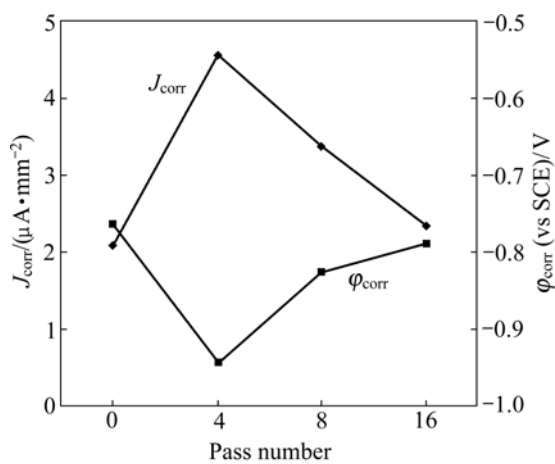


Fig.4 Corrosion characteristics of as-cast and ECAPed Al-23%Si alloy with various passes

The corrosion data of ECAPed samples obtained from immersion are listed in Table 1. It is clear that the mass-loss ratio of ECAPed samples obviously decreases with increasing the pass number of ECAP. The mass-loss ratio of the 16-pass ECAPed sample is lowered to 28.7% that of the 4-pass ECAPed sample and 36.4% that of the 8-pass ECAPed sample. This is consistent with the foregoing results of potentiostatic polarization tests in neutral NaCl solution.

Table 1 Mass-loss ratios of ECAPed samples in 0.6 mol/L NaCl solution at room temperature

Pass number	4	8	16
Mass-loss ratio/($\text{mg} \cdot \text{m}^{-2} \cdot \text{h}^{-1}$)	91.5	72.2	26.3

Fig.5 shows the SEM morphologies of the corroded surface of the ECAPed Al-23%Si alloys after immersion for 80 h, with (a), (b) and (c) for 4-, 8- and 16-pass ECAPed samples, respectively. It is obvious that the 4-pass ECAPed sample has much more corroded spots on the surface and higher pitting tendency than others. With increasing the ECAP passes to 16, the corroded spots of the ECAPed sample become smaller in size and less in quantity. Fig.5(d), a high magnification image of the pitting corroded area signed in Fig.5(a), shows that the corrosion occurs in the congregation area of silicon particles. During the primary ECAP passes, large primary silicon particles are broken into smaller particles, but these particles are still assembled around the primary silicon particle. In addition, there are many biggish voids produced due to the primary silicon breaking during ECAP processing, as shown in Figs.1(b) and (e). These areas containing biggish voids are very weak in the corrosion solution. This should be the reason that the corrosion occurs in the silicon congregation areas. With increasing ECAP passes, the assembled silicon particles are dispersed homogenously into aluminum alloy matrix and the voids gradually become less, as shown in Figs.1(c), (d) and (f). Therefore, the corrosion resistance of this alloy is improved, as shown in Figs.5(b) and (c), and the corroded spots become less and smaller with the increase of ECAP passes.

From the results of electrochemical analysis, immersion test and SEM observations, corrosion resistance of ECAPed Al-23%Si alloy decreases after the first 4 passes, then is improved gradually by increasing pressing passes. Clearly, these features are attributed to microstructure characteristics of the ECAPed samples. As shown in Fig.1, the as-cast Al-23%Si alloy consists of large aluminum dendrites, eutectic silicon crystals and large primary silicon crystals with polygonal shapes. When this alloy is immersed in neutral NaCl solution, its natural alumina film would be dissolved to a certain degree and induce the formation of localized galvanic cells between cathodic silicon crystals and anodic Al matrix. Therefore, the as-cast sample is generally eroded with coincident pitting corrosion due to its inhomogeneous microstructure.

During 4-pass ECAP, a large number of primary silicon particles are broken while many biggish voids are formed around the brittle silicon particles, which results

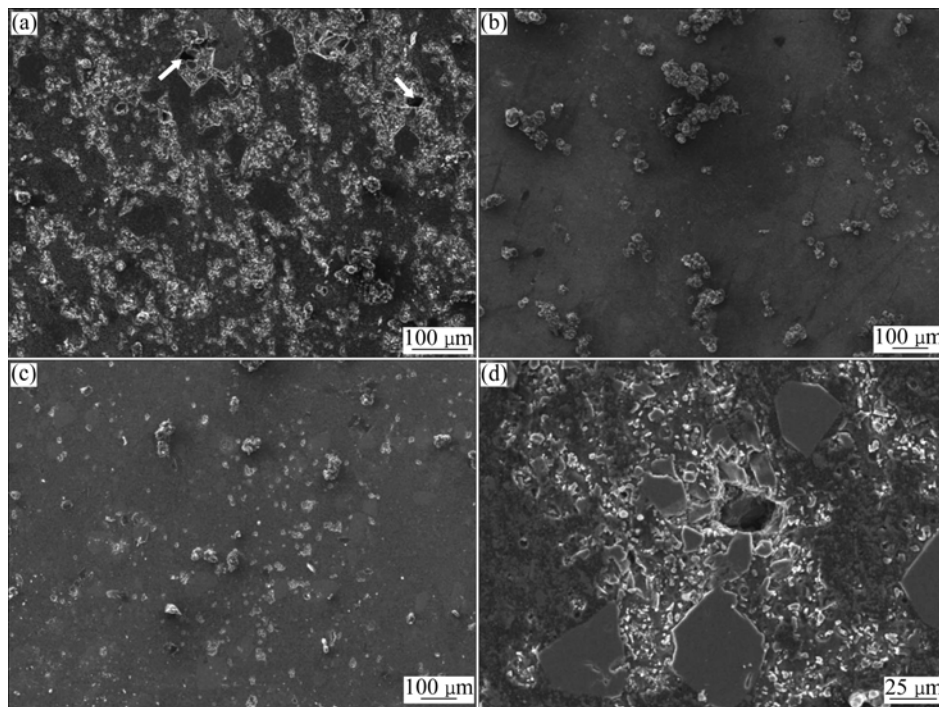


Fig.5 SEM images of corroded surface morphologies of ECAPed Al-23%Si alloy after immersion test for 80 h: (a) 4 passes; (b) 8 passes; (c) 16 passes; (d) High magnification of pitting area in (a)

in higher pitting susceptibility and general galvanic corrosion rate. With increasing ECAP passes, the primary silicon particles are progressively broken into fine particles and homogeneously dispersed in the ultrafine-grained aluminum matrix while the voids noticeably evanesce. Obviously, the small size of cathode phases promotes micro-galvanic cells to be established more numerous and uniformly, which reduces the susceptibility of pitting corrosion in “small cathode, large anode” mechanism. That is to say, the UFG sample with fine particles and few small voids inclines to general corrosion. Therefore, it is feasible to improve the corrosion resistance of Al-23%Si alloy, even go beyond that of as-cast alloy, by increasing the ECAP passes for getting ultrafine aluminum grains and fine silicon particles in homogenous distribution without voids. The result indicates that, besides excellent mechanical properties[15], enough ECAP passes are beneficial to increasing corrosion resistance of hypereutectic Al-23%Si alloy.

Noticeably, some available investigation, such as BALYANOV et al[18], HADZIMA et al[19] and CHUNG et al[22], did not find out the disadvantage of ECAP in initial passes to corrosion resistance because those materials are more plastic than Al-23%Si casting alloy.

4 Conclusions

1) As-cast Al-23%Si alloy was processed through

multi-pass ECAP to determine the corrosion behavior of UFG microstructure after severe plastic deformation. The corrosion resistance of ECAPed alloy is decreased after the initial 4 passes and then is improved with more pressing passes. The 16-pass ECAPed sample has the ϕ_{corr} and J_{corr} values similar to the as-cast alloy, and a quite low mass-loss ratio compared with the 4-pass ECAPed sample in neutral NaCl solution.

2) Higher pitting susceptibility of the ECAPed Al-23%Si alloy after initial 4 passes is due to the presence of biggish voids around the brittle primary silicon crystals broken during ECAP. After more ECAP passes, the voids become less and the congregated silicon particles are homogeneously dispersed. This indicates that the pitting resistance of the 16-pass ECAPed sample is higher than that of the 4-pass ECAPed sample, in accordance with SEM images of the corroded surface morphologies.

3) UFG aluminum alloy with many fine silicon particles and few small voids inclines to general corrosion. Besides excellent mechanical properties, enough ECAP passes are beneficial to increasing corrosion resistance of hypereutectic Al-Si alloy with homogenous distribution of fine silicon particles on ultrafine matrix grains and gradual elimination of voids derived from the primary silicon particles.

References

[1] CHEN Z H, KANG Z T. Solid liquid mixed casting of Al-Si alloy [J].

- Journal of Central South University of Technology, 2000, 7(3): 133–135.
- [2] FRANK SU Y H, SAM CHIANG C S, TSAO C Y A. Extrusion characteristics of spray-formed AC9A aluminum alloy [J]. *Materials Science and Engineering A*, 2004, 364: 305–312.
 - [3] SHIBATA S, TOMITA S, NAKATA K. Surface modification of hypereutectic aluminum alloys by laser beam remelting [J]. *Journal of Japan Institute of Light Metals*, 2000, 50: 609–615.
 - [4] MATSUURA K, SUZUKI K, OHMI T, KUDOH M, KINOSHITA H, TAKAHASHI H. Dispersion strengthening in a hypereutectic Al-Si alloy prepared by extrusion of rapidly solidified powder [J]. *Metallurgical and Materials Transactions A*, 2004, 35A: 333–339.
 - [5] SITDIKOV O, SAKAI T, AVTOKRATOVA E, KAIBYSHEV R, KIMURA Y, TSUZAKI K. Grain refinement in a commercial Al-Mg-Sc alloy under hot ECAP conditions [J]. *Materials Science and Engineering A*, 2007, 444(1/2): 18–30.
 - [6] JIANG Ju-fu, LUO Shou-jing. Microstructure evolution of processed Mg-Al-Zn alloy by equal channel angular extrusion in semi-solid isothermal treatment [J]. *Transactions of Nonferrous Metals Society of China*, 2006, 16(6): 1313–1319.
 - [7] HWANG B, LEE S, KIM Y C, KIM N J, SHIN D H. Microstructural development of adiabatic shear bands in ultra-fine-grained low-carbon steels fabricated by equal channel angular pressing [J]. *Materials Science and Engineering A*, 2006, 441(1/2): 308–320.
 - [8] WEI W, CHEN G, WANG J T, CHEN G L. Microstructure and tensile properties of ultrafine grained copper processed by equal-channel angular pressing [J]. *Rare Metals*, 2006, 25(6): 697–703.
 - [9] MA A B, SUZUKI K, NISHIDA Y, SAITO N, SHIGEMATSU I, TAKAGI M, IWATA H, WATAZU A, IMURA T. Impact toughness of an ultrafine-grained Al-11mass%Si alloy processed by rotary-die equal-channel angular pressing [J]. *Acta Materialia*, 2005, 53: 211–220.
 - [10] MA A B, TAKAGI M, SAITO N, IWATA H, NISHIDA Y, SUZUKI K, SHIGEMATSU I. Tensile properties of an Al-11mass%Si alloy at elevated temperatures processed by rotary-die equal-channel angular pressing [J]. *Materials Science and Engineering A*, 2005, 408: 147–153.
 - [11] KIM W J, HYUN C Y, KIM H K. Fatigue strength of ultrafine-grained pure Ti after severe plastic deformation [J]. *Scripta Materialia*, 2006, 54: 1745–1750.
 - [12] KAPOOR R, LI Y J, WANG J T, BLUM W. Creep transients during stress changes in ultrafine-grained copper [J]. *Scripta Materialia*, 2006, 54: 1803–1807.
 - [13] FIGUEIREDO R B, LANGDON T G. The development of superplastic ductilities and microstructural homogeneity in a magnesium ZK60 alloy processed by ECAP [J]. *Materials Science and Engineering A*, 2006, 430: 151–156.
 - [14] STOLYAROV V V, GUNDEROV D V, POPOV A G, PUZANOVA T Z, RAAB G I, YAVARI A R, VALIEV R Z. High coercive states in Pr-Fe-B-Cu alloy processed by equal channel angular pressing [J]. *Journal of Magnetism and Magnetic Materials*, 2002, 242/245: 1399–1401.
 - [15] MA A B, SUZUKI K, SAITO N, NISHIDA Y, TAKAGI M, SHIGEMATSU I, IWATA H. Impact toughness of an ingot hypereutectic Al-23mass% Si alloy improved by rotary-die equal-channel angular pressing [J]. *Materials Science and Engineering A*, 2005, 399: 181–189.
 - [16] VINOGRADOV A, MIMAKI T, HASHIMOTO S, VALIEV R Z. On the corrosion behaviour of ultra-fine grain copper [J]. *Scripta Materialia*, 1999, 41: 319–326.
 - [17] ROFAGHA R, LANGER R, EI-SHERIK A M, ERB U, PALUMBO G, AUST K T. The effects of grain size and phosphorus on the corrosion of nanocrystalline Ni-P alloys [J]. *Nanostructured Materials*, 1993, 2: 1–10.
 - [18] BALYANOV A, KUTNYAKOVA J, AMIRKHANOVA N A, STOLYAROV V V, VALIEV R Z, LIAO X Z, ZHAO Y H, JIANG Y B, XU H F, LOWE T C, ZHU Y T. Corrosion resistance of ultra fine-grained Ti [J]. *Scripta Materialia*, 2004, 51: 225–229.
 - [19] HADZIMA B, JANEČEK M, ESTRIN Y, KIM H S. Microstructure and corrosion properties of ultrafine-grained interstitial free steel [J]. *Materials Science and Engineering A*, 2007, 462: 243–247.
 - [20] NISHIDA Y, ARIMA H, KIM J C, ANDO T. Rotary-die equal-channel angular pressing of an Al-7mass%Mg alloy [J]. *Scripta Materialia*, 2001, 45: 261–266.
 - [21] LI Jiu-qing, DU Cui-wei. Experimental methods and inspection technologies of corrosion [M]. Beijing: China Petrochemical Press, 2007: 5. (in Chinese)
 - [22] CHUNG M K, CHOI Y S, KIM J G, KIN Y M, LEE J C. Effect of the number of ECAP pass time on the electrochemical properties of 1050 Al alloys [J]. *Materials Science and Engineering A*, 2004, 366: 282–291.

(Edited by YANG Bing)